CrossMark

ORIGINAL PAPER

Quantification and Reduction of the Residual Chemical Reactivity of Passivated Biodegradable Porous Silicon for Drug Delivery Applications

Q. Shabir[1] ⦿ · K. Webb[1] · D. K. Nadarassan[1] · A. Loni[1] · L. T. Canham[1] ·
M. Terracciano[2,3] · L. De Stefano[2] · I. Rea[2]

Abstract The chemical reactivity of as-anodized porous silicon is shown to have an adverse effect on a model drug (Lansoprazole) loaded into the pores. The silicon hydride surfaces can cause unwanted reactions with actives during storage or use. Techniques such as thermal oxidation or surface derivatization can lower the reactivity somewhat, by replacing the reactive silicon-hydride species with a more benign oxide or functional group. However, by using a trio of analytical techniques (fluorometric dye assay, HPLC assay, and chemography) we show that residual hydride is still likely to be present and only after combining thermal oxidation with surface derivatization can the residual reactivity be reduced to those values typically observed with sol-gel (porous) silica. Potential sources of residual reactivity are discussed, with reference to data obtained by trace metal analysis, residual solvents, and pH measurements.

Keywords Porous silicon · Reactivity · Derivatization · Drug delivery

✉ Q. Shabir
  qshabir@psivida.com

[1] pSiMedica Ltd, Malvern Hills Science Park, Geraldine Road, Malvern, Worcester WR14 3SZ, UK

[2] Institute for Microelectronics and Microsystems, National Research Council, Via P. Castellino 111, 80131, Naples, Italy

[3] Department of Pharmacy, University of Naples Federico II, via D. Montesano 49, 80131, Naples, Italy

1 Introduction

Porous silicon has been under pre-clinical evaluation for drug delivery for a number of years [1–6]. Its medical biodegradability and biocompatibility [7–9], widely tuneable pore sizes via electrochemical etching [10, 11], flexible surface chemistry [12, 13] and high payloads of nanostructured drugs [14] are its key attributes in this regard. However, biodegradable materials are generally, almost by definition, more chemically reactive than "bio-inert" ones. Biodegradable polymers, for example, liberate acidic by-products that are well known to introduce local pH changes that can damage the tertiary structure of large biomolecules like proteins [15, 16]. Biodegradable metal degradation products, like hydrogen gas from magnesium, may cause adverse reactions *in vivo* [17] and may lead to body fluid alkalization locally [18].

Biodegradable semiconducting silicon degrades into orthosilicic acid *in vivo,* which is naturally present in the human body [19], but can also release trace levels of silane [20] and can contain residual silicon-hydride bonds after thermal passivation (oxidation) treatments (21). If insufficient post-etch rinsing and drying is carried out the material can also contain sufficient HF-based electrolyte, solvent residues and etch by-products to cause cytotoxicity and reactivity [22]. Pharmacopeia requirements for drug formulations include very low levels of "Active Pharmaceutical Ingredient" (API) modification during long term storage (e.g. <5% over 6 months). This necessitates modifying the vehicle or carrier if it interacts with API chemistry. In the case of mesoporous silicon, optimizing the pore wall chemistry to minimize any chemical reactions with the entrapped drug molecules is a prerequisite before loading it with active molecules.

Porous silicon is commonly manufactured by the etching of crystalline silicon in aqueous and non-aqueous electrolytes containing hydrofluoric acid [23]. The surface of freshly prepared porous silicon is covered with a layer of Si-H bonds with minor quantities of Si-F and Si-O species also present. The reactivity of as-etched porous silicon is dominated by the chemistry of Si-Si and Si-H bonds [12] particularly when trying to load biomolecules or actives in pores for drug delivery. As etched (as-anodized) porous silicon contains a high concentration of silicon hydride bonds at its surface; which act as a reducing agent. Therefore to make the material non-reactive with APIs, the Si-H bonds are oxidized to yield a passivated product, which is less reactive due to lower amounts of hydrides [20, 21]. Derivatization of Si-H bonds with aminosilane compounds like APTES or APDMES has also been employed to make the pore wall surface more stable and more compatible with biomolecules such as oligonucleotides [24].

In the present study, reactions of residual hydride of thermally annealed, oxide-passivated, derivatized or both oxidized and derivatized porous silicon samples were studied using three distinct assays. The first of these is a chemical method based on hydride-mediated degradation of the Lansoprazole drug, a substituted 2-(2-pyridylmethyl) sulfinyl benzimidazole molecule, used as a PPI (proton pump inhibitor) in the inhibition of gastric acid secretion. Lansoprazole shows high sensitivity to proton attack at the sulfoxide group under weak acidic conditions [25]. Silicon hydride bonds at the pore wall surface act as a reducing agent when in contact with the Lansoprazole molecule. This reducing effect on Lansoprazole is proportional to the hydride content of the porous silicon material and the drug will degrade in the reaction mixture accordingly. The percentage of degraded Lansoprazole can be used as a direct measurement of the chemical reactivity of the porous silicon.

A second method also uses a hydride-mediated oxidation reduction of phenoxazin-3-one dyes Resazurin and Resorufin [26]. In this assay, hydride from porous silicon reduces the weakly fluorescent dye Resazurin to the highly fluorescent molecule Resorufin at pH 7.6 in phosphate buffer [27]. At the emission peak of Resorufin (587 nm), fluorescence from Resazurin is negligible and is used as a blank in the assay procedure.

The third approach for reactivity assessment is chemographic analysis of the samples. Porous silicon releases low levels of gaseous silanes in humid air which create images on photographic plates through reduction of the silver halide in a photographic emulsion [28]. The low levels of monosilane emission are thought to be primarily due to hydrolysis of $Si-H_3$ bonds, so relatively high concentrations of hydrides on the surface will cause the chemographic effects to be more pronounced for as-etched material

than oxide-passivated or derivatized porous silicon surfaces [29].

We believe that these three methods complement each other in analyzing the residual hydrides within porous silicon post oxide-passivation or derivatization, so they were simultaneously used following a variety of chemical passivation treatments on a specific porous silicon structure, in order to quantitatively compare the resulting residual reactivity.

2 Materials and Methods

2.1 Reagents

3-aminopropyltriethoxysilane (APTES), 3-aminopropyltriethoxysilane (APDMES), 1-decene, Resazurin, Resorufin and Lansaprazole were purchased from Sigma Aldrich. All other solvents and buffers were purchased from Sigma and were research-grade chemicals.

2.1.1 Manufacture of Porous Silicon Particles

Porous silicon microparticles were prepared from six inch diameter p^+ wafers (boron-doped, resistivity range 0.005-0.02 Ω.cm) via anodization in an HF-methanol based electrolyte. Current density and time were chosen to yield two forms of free-standing mesoporous silicon layers: (a) average porosity of 86% and 227 μm thickness (sample BS419) and (b) average porosity of 68% and 150 μm thickness (sample BS445); after rinsing and drying, the higher-porosity samples were ball-milled at 300 rpm in air for 1min, then passed through a 53 μm stainless steel sieve to obtain a powder with a defined particle size distribution (Table 1); samples BS419 were subsequently oxidized at 700 °C for 16 hours in a Carbolite HTR 11/75 rotary furnace and then hydrated in deionized water before drying under vacuum overnight. The lower-porosity samples (BS445) were rotor-milled at 20,000 rpm to yield powder with a size distribution and gas adsorption properties shown in Table 1.

2.1.2 Characterization of Porous Silicon Particles

Porous silicon particle size was measured using the Mastersizer 2000 laser diffraction system with a Hydro MU dispersion unit. The material was wet to a paste with 5% (w/w) Igepal CA (aq) before being dispersed in deionized water for measurement. The raw scattering data was deconvolved using Mie theory and an average particle size distribution was generated from five measurements.

Gas adsorption analysis on the porous silicon powders was conducted with nitrogen and a Micromeritics TriStar

Table 1 Physicochemical properties of oxidized porous silicon microparticles prior to derivatization treatments

Property	Milled pSi (BS445)	Milled & Oxidised pSi (BS419)
Particle size distribution	d10 = 1.5 μm; d50 = 17.8 μm; d90 = 44.2 μm	d10 = 3.9 μm; d50 = 15 μm; d90 = 43 μm
Surface area (m^2/g)	287	217
Pore volume (ml/g)	0.994	0.969
Pore size (APD in nm)	13.7	16.6
pH[a]	Not measured	4.1 +/- 0.2
Residual solvents[a] (ethanol/methanol)	Not measured	<1000 ppm
Heavy metal impurities (class 1)[a]	Not measured	None detected (XRF)
Heavy metal impurities (class 2)[a]	Not measured	Cu (17-22 ppm), Ni (11-12 ppm)

[a]Data from other batches made under nominally similar conditions

3000 system. Computational analysis of the isotherms yielded absolute values for surface area (based on the Brunauer-Emmett-Teller/BET method), pore volume (based on the Barrett-Joyner-Halenda/BJH method) and average pore diameter (APD from BJH adsorption data).

Chemical purity with respect to trace heavy metals was assessed in selected batches via X-ray fluorescence (XRF) carried out using a Bruker S8 Tiger spectrometer with a semi-quantitative software analysis suite. 1 g batches of material were loaded into aluminum sample cups and held in place with an ultrathin Mylar film.

Residual solvent levels (ethanol and methanol) in selected batches were quantified with a PerkinElmer Autosystem XL Gas Chromatography system with a BP-624 capillary column following the pharmacopeia protocol USP/NF 467.

pH was determined using the pharmacopeia protocol USP/NF 791 wherein a suspension of 0.2 g +/- 0.01 g material is sonicated for 1 minute in 5.0 ml of carbon-dioxide free water. Measurements were conducted on a calibrated Mettler Toledo MP225 pH meter at 25+/- 2 °C.

FTIR was conducted on a Nicolet Continu μm XL Thermo Scientific, equipped with a microscope; measurements were performed in reflection mode on an area of 100 × 100 μm^2. The number of scans was set to 64. Spectra were collected in the range of 4000–500 cm^{-1} with a resolution of 2 cm^{-1}.

Surface charge measurements of bare and functionalized porous silicon nanoparticles were carried out by dynamic light scattering (DLS) using a Zetasizer Nano ZS (Malvern Instruments, Malvern, UK).

2.1.3 Hydrosilylation of Porous Silicon Particles

Porous silicon microparticles were placed in a Schlenk tube containing a deoxygenated neat 1-decene (99% v/v) and allowed to react at 110 °C for 18 h under a stream of argon (Fig. 1, II, III).

Microparticles were extensively washed in tetrahydrofuran and chloroform so as to remove excess of unreacted and physisorbed reagent. Microparticles dispersion was centrifuged at each wash for 30 min at 13,000 rpm and the supernatant was discarded.

2.1.4 Silanization of Porous Silicon Particles

The functionalization procedure is based on silane chemistry. PSi-NPs were treated with Piranha solution (H_2O_2:H_2SO_4 1:4), in order to create OH groups, for 30 minutes at ambient temperature. After treatment with the Piranha solution, samples were extensively washed in milli-Q® water to remove any adsorbed acid (Fig. 1, I). The microparticle dispersion was centrifuged for 30 minutes at 13,000 rpm and the supernatant was discarded. The pellet was silanized by immersion in 5% aminosilane solution; APTES or APDMES in dry ethanol for 1 hour at room temperature. After silanization, samples were extensively washed in dry ethanol and then centrifuged for 30 min at 13,000 rpm and the supernatant discarded. The pellet was incubated for 10 minutes at 100 °C (curing process).

2.1.5 Chemical Reactivity of Porous Silicon by RP-HPLC Method

HPLC was performed using an Agilent 1200R series with a C18 bonded stationary phase. The separation was achieved with an ACE C18 (150 × 4.6 mm) column. Solvent A consisted of water and solvent B consisted of acetonitrile: water: triethylamine (80: 20: 0.005), the pH of solvent B was adjusted to 7 with orthophosphoric acid (85% v/v). These solutions were used to set up a gradient elution method. The mobile phase is run through the column on a linear gradient of increasing organic modifier; flow rate was set at 0.8 mL/min and the eluent was monitored at 285 nm.

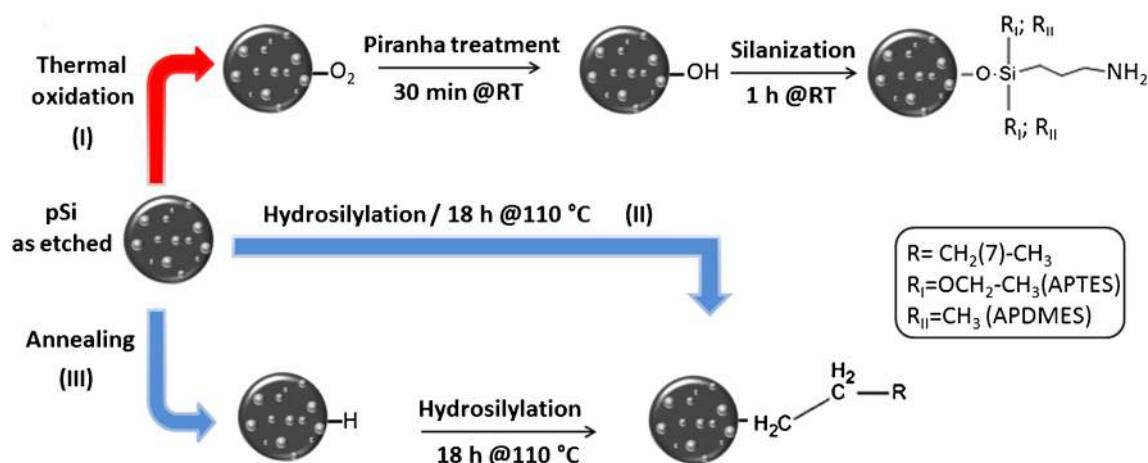Lansoprazole is separated from its associated degradation products according to the RP-HPLC method described

Fig. 1 Thermal and chemical passivation of porous silicon powders: (*I*) thermal oxidation and BS419 silanization process by APTES or APDMES; (*II*) BS445 chemical passivation by hydrosilylation with 1-decene; (*III*) BS445 annealing and hydrosilylation by 1-decene

in the United States Pharmacopeia [30] for this molecule. The Lansoprazole solution was accurately prepared at an API concentration of 10 mg/mL in methanol. Each sample required 100 μL of the Lansoprazole solution. Approximately 20 mg ($\pm$ 2 mg) of each silicon /silica sample was weighed in duplicate into a 5 mL freeze drying vial. Approximately 100 μL of the Lansoprazole/methanol solution was added to the samples and sealed with a butyl stopper and aluminum overseal. The samples were placed in a 25 °C water bath and incubated for 2 hours. As a control sample, 100 μL of the Lansoprazole/methanol solution was pipetted into a 5 mL freeze drying vial and incubated alongside the other samples. As-anodized porous silicon was used as a positive control which showed maximum degradation of the drug compared with other samples.

After incubation, the overseal and the stopper were removed, taking care as the vial may contain gas as a result of any reactivity associated with the porous silicon. Each sample and the Lansoprazole control was diluted with 4.9 mL methanol and gently mixed. The porous silicon was allowed to settle, and then 1 mL of the supernatant was removed and filtered into a HPLC vial using a Whatman 0.2 μm PVDF filter.

Each sample was assayed by RP- HPLC (25, 30) to determine the total percentage of degradation in the samples in comparison to the control (Lansoprazole in methanol) solution. The method was validated for specificity and reproducibility.

2.1.6 Dye Reactivity by Fluorimetric Method

A PerkinElmer 1420 Victor3 Multilevel Counter was used to quantify the highly fluorescent pink Resorufin dye which is produced by reduction of blue Resazurin by hydride

surfaces of porous silicon. Fluorescence measurements utilized a CW lamp filter of 531 nm (excitation) and emission filter of 616 nm for quantification. (Alamar Blue assay, US patent No5, 501,959).

About 15% solutions of Resazurin and Resorufin were prepared in 50 mM phosphate buffer pH7.6. From the stock solution of Resorufin various dilutions were made in phosphate buffer (pH7.6) to achieve a sufficient number of solutions within the concentration range 0-2.0 μg/mL for the generation of a standard calibration plot.

From the 15% solution of Resazurin, a 2.5 μg/mL working solution was prepared in the same phosphate buffer (pH7.6). Duplicate samples of 20 $\pm$ 0.5 mg pSi were weighed into amber Eppendorf tubes. About 1 mL of the 2.5 μg/mL working Resazurin dye solution was added to each silica/silicon sample to give a suspension of 20 mg/mL. After two hours of incubation at 25 °C, the Eppendorf tubes were centrifuged at 14000 rpm for 2 minutes and 200 μL of the supernatant liquid was transferred to a 96 well plate in triplicate. The fluorescence values of each sample were compared to that of the blue Resazurin dye solution, to that of silica which has no hydride bonding and to that of 500 °C oxidized pSi which has a significant number of hydrides but still can be wetted with the buffer.

2.1.7 Chemographic Method:

Chemography utilized 25 μm thick Ilford L4 nuclear tracking emulsion plates with a custom built light-tight box wherein there was 100% humidity at 25 °C.

Porous silicon powders (20 mg) which were as-etched, oxide passivated or derivatized were weighed and then placed in direct contact with the nuclear emulsion plate in air of 100% relative humidity at 25 °C for times ranging

from 10 minutes to 100 hours in complete darkness. The position of the powders was recorded by photography prior to plate exposure. After exposure, the plates were soaked in Ilford developer for 2 minutes, soaked in Ilford stop solution for 1 minute and fixed in Ilford fixer for 15 minutes. All of these operations were conducted at 25 °C. Subsequent plate washing in stream of water for 15 minutes was again carried out at room temperature.

2.2 Results

2.2.1 Derivatization of pSi Particles

Porous silicon particles surface chemistry has been modified in three different ways, sketched in Fig. 1: the first route is a three-step procedure which starts with a thermal oxidation in wet atmosphere at 400 °C, followed by an activation in Piranha solution and a silanization of powders that leads to an amino-terminated surface; the second is a direct passivation of the pSi surface in pure 1-decene which gives a Si-C surface; the third is thermal annealing in inert atmosphere at 400 °C plus hydrosilylation, having the same result as route (II).

The passivation treatments of pSi powders were analysed by FTIR spectroscopy. In Fig. 2 and Table 2 the spectra changes of SiH and annealed SiH powders after thermal hydrosylilation by 1-decene are reported: the comparison between FTIR spectra before and after treatments, confirmed an almost complete conversion of pSi particle surface chemistry. The evidence is the presence of characteristic peaks of Si-C covalent bond: stretching modes of C–H$_x$ bonds at 2957-2853, 1465-1368 and 725-720 cm^{-1}. However, all FTIR spectra showed a weak characteristic peak of backbone Si–H bonds at 2100 cm^{-1} and the peak of

Table 2 FTIR peak values of porous silicon powders (BS419) after hydrosilylation process

SiH/ Hydrosilylated SiH Annealed SiH/ Hydrosilylated SiH
a 1= 2957-2853 cm^{-1} CHx asymmetric stretch
a 2= 1456-1368 cm^{-1} CHx symmetric stretch
a 3= 725-720 cm^{-1} CH stretch
b= 2100 cm^{-1} Si-H stretch
c= 1090-1100 cm^{-1} Si-O-Si stretch

Si–O–Si stretching mode at 1090-1100 cm^{-1} probably due to spontaneous ageing of pSi powders during the handling.

FTIR spectra of SiH and SiO$_2$ powders, in Fig. 3 and Table 3, confirmed the success of silanization: both samples showed the peaks at 1655 and 1550 cm^{-1}, corresponding to the bending mode of the free NH$_2$ groups, the CH$_x$ asymmetric/CH$_2$ deformations at 2925, 1368 and 780 cm^{-1}, a peak of Si–O–Si stretching mode due to Piranha treatment for SiH and thermal oxidation for SiO$_2$ at 1090-1010 cm^{-1}. In the case of the SiH sample, the characteristic peak of backbone Si–H bonds at 2100 cm^{-1} was also observed. FTIR characterization cannot show structural differences between APTES and APDMES: the two compounds have the same alkyl chain but while APTES has three ethoxy groups, that cause polymerization of compound and thus a better coverage of surface, APDMES instead has two
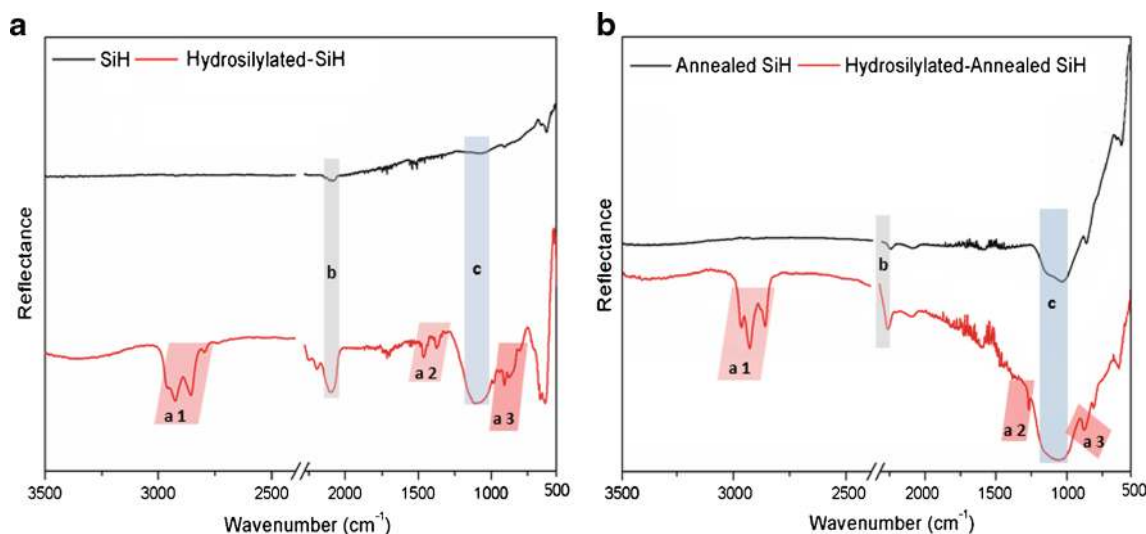

Fig. 2 FTIR spectra of pSi powders (BS419) before and after the hydrosilylation (**a**) and after annealing and *hydrosilylation (**b**)*
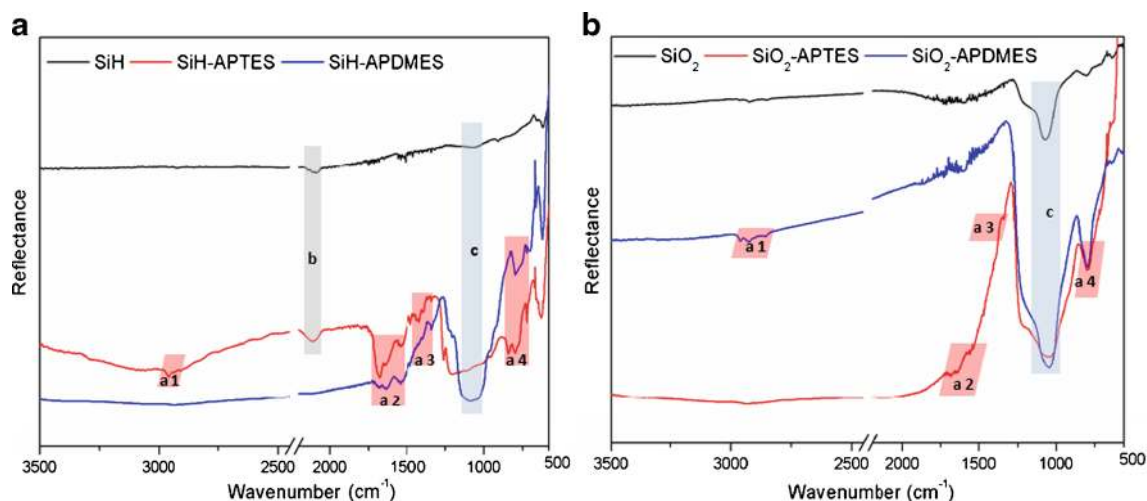
Fig. 3 FTIR spectra of porous silicon BS419 (**a**) and oxidized porous silicon BS445 (**b**) powders before and after the silanization with APTES and APDMES

methyl groups and one ethoxy group and does not polymerize. The DLS measurements confirmed the correct functionalization of particles surface due to a change of sample zeta potential from -16 ($\pm$ 4) mV to +7 ($\pm$ 3) mV after silanization.

2.2.2 HPLC Based Chemical Reactivity Assay

When incubated with 20 mg of as-etched pSi, the Lansoprazole-methanol solution showed a maximum degradation of 30% compared with a 20 mg sample of commercially available porous silica (Davisil, 60Å) where degradation is less than 0.02% (Fig. 4). Previous results have shown that when the Lansoprazole-methanol solution was incubated with samples of thermally passivated pSi, the proportion of Lansoprazole degradation was seen to decrease as the temperature used to passivate the silicon skeleton was increased over the range 500-800 °C [49].

Table 3 FTIR peak values of porous silicon/silica powders after silanization

SiH-APTES/APDMES SiO₂ -APTES/APDMES
a 1= 2925 cm⁻¹ CHx asymmetric stretch
a 2= 1368 cm⁻¹ CHx symmetric stretch
a 3= 1655–1550 cm⁻¹ NH bend
a 4 = 1368-780 cm⁻¹ CH stretch
b = 2100 cm⁻¹ Si-H stretch
c = 1090-1100 cm⁻¹ Si-O-Si stretch

The Lansoprazole mediated degradation of oxide-passivated and derivatized samples is shown in Table 4. Biosilicon material (BS445) that was passivated at 400 °C and annealed in the presence of nitrogen was found to be highly reactive. This batch showed almost complete degradation (95%) of Lansoprazole; more than 65% than the as-anodized control batch which degrades Lansoprazole by 28-30%. The hydrosilylation of anodised batches reduced degradation significantly to 12.32% whereas hydrosilylation and annealing further reduced it to 3.95%. Derivatization of anodised batch with APDMES resulted in a slight decrease in degradation, while with APTES the reactivity was seen to lower significantly (0.58%). pSi samples (BS419) which have been oxide-passivated at 700 °C for more than 16 hours and then derivatized showed low reactivity values of <1%.

Table 4 shows HPLC measurement of surface reactivity of porous silicon powders (BS419 & BS445) after varied treatments.

2.3 Dye Based Reactivity Assay

A fluorimetric dye method was used for measuring the reactivity of porous silicon samples. Chemical reactivity of porous silicon has been ascribed to hydrides associated with the surfaces of the particles (12,21). These hydride surfaces reduce Resazurin (blue), a marginally fluorescent dye, to pink Resorufin which is highly fluorescent.

A linear relationship between Resorufin concentration and fluorescence was seen over the concentration range from 0.07-1.68 μg/mL with an R2 value of 0.9965 (Fig. 5). This standard plot was used to quantify the amount of Resazurin converted to Resorufin due to the presence of hydride bonds at the surface. The method was validated

Fig. 4 Chromatograms of (**a**) free Lansoprazole and Lansoprazole following incubation with (**b**) commercial sol-gel SiO$_2$ (**c**) unpassivated porous silicon
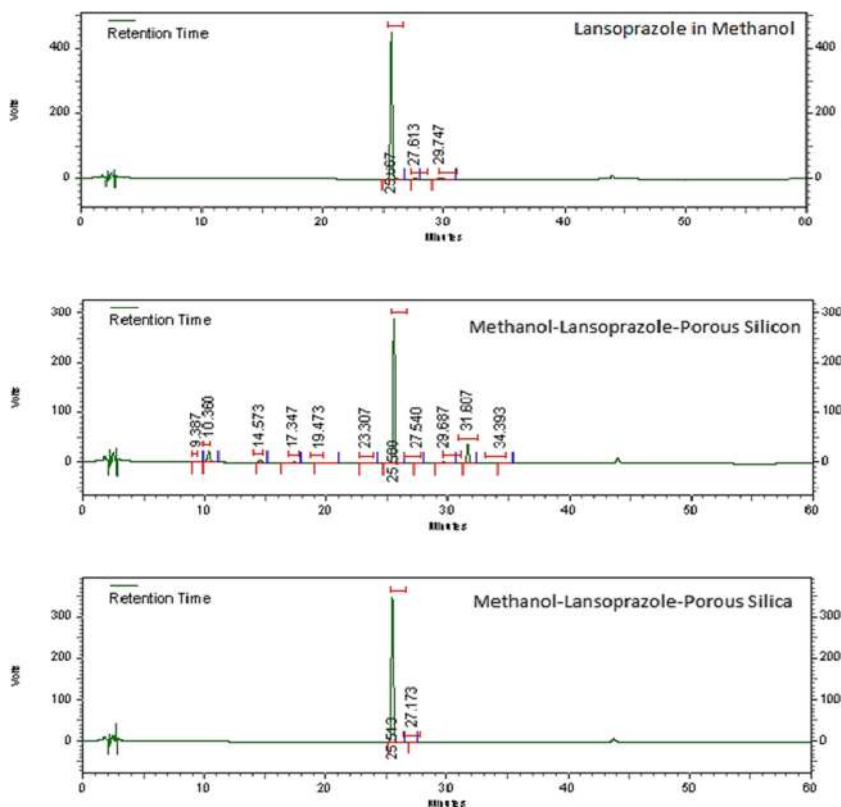
for accuracy, linearity and specificity. Potential interference from the derivatization reagents (APTES, APDMES and decene) on the fluorescence assay was found to be negligible or within the acceptable limits of a fluorimetric assay for all three reagents (Table 5).

The amount of Resorufin produced can be used as a direct measurement of the chemical reactivity of the sample. As-anodized or native oxide passivated pSi samples cannot be analysed by this assay due to poor wettability; therefore slightly passivated controls (500 °C for 1 hour) are used as a positive control in this assay. When 20 mg of this form of pSi was incubated with 1ml of (2.5 μg/ml) Resazurin, approximately 2.2-2.4 μg/mL of

Resorufin was measured. Incubation with porous silica on other hand generates only 0.01 μg/mL of Resorufin under similar conditions. The dye based data on reactivity of pSi samples are shown in Table 5. With hydrosilylated pSi samples (as with HPLC) it was noted that APDMES derivatized samples showed higher reactivity compared with derivatization by APTES. While hydrosilylation alone did not reduce the reactivity significantly, annealing and hydrosilylation proved to reduce the hydride content more effectively. Oxidized batches showed significantly lower reactivity after hydrosilylation with APDMES and the improvement is even more pronounced after hydrosilylation with APTES.

Table 4 HPLC measurement of surface reactivity of porous silicon powders (BS419 & BS445) after varied treatments

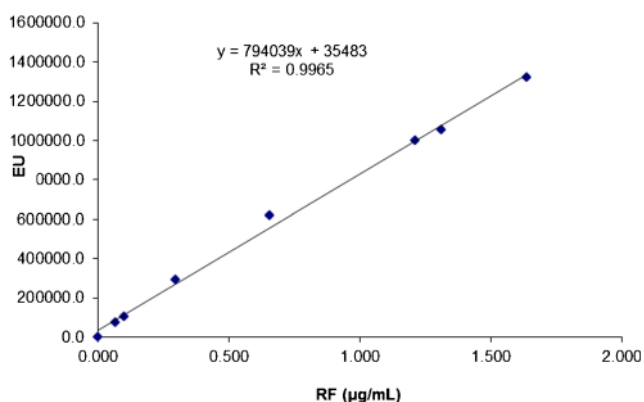| Sample	Chemical passivation treatments	Degradation of Lansoprazole post incubation (%)
BS445	Si-H annealed (400°C in nitrogen)	94.9
BS445	Si-H & APDMES	16.51
BS445	Si-H & hydrosilylation	12.32
BS445	Si H-annealed & hydrosilylation	3.95
BS419	Si-H & oxidation & APDMES	0.64
BS445	Si-H & APTES	0.58
BS419	Si-H & oxidation	0.54
BS419	Si-H & oxidation & APTES	0.30
	Sol gel silica (control)	0.01

Fig. 5 Relationship of Fluorescence (*y-axis*) to Resorufin Concentration (*x-axis*)

2.3.1 Chemography Results

As-etched pSi can generate darkening on a photographic plate within 10 minutes exposure (28). When as-etched pSi and 800 °C passivated (rotary furnace, 16 hours) pSi were exposed for 4 hours at 100% humidity, only as-etched pSi showed a dark spot while the oxidized sample showed no image, indicating that the rate of silane emission from this sample is much slower or negligible (Fig 6). While hydrosilylated samples showed a strong image after 20 hours, pSi treated with APTES and APDMES showed a faint image after 20 hours which was stronger after 72 to 100 hours. Samples which were passivated for 700 °C for 16 hours showed a faint image after 100 hours, which was completely absent after additional hydrosilylation with APTES or APDMES.

Figure 6 provides an example of the chemographic effects seen and summarized in Table 6. Figure 6a shows the image of powders before exposing them to photographic film and Fig. 6b shows a strong image seen from the Si-H hydrosilylated sample; a faint image seen from the Si-H APDMES sample; and no image seen from Si-H & APTES and Si-H annealed samples.

Table 5 Dye reactivity of porous silicon powders (BS419 & BS445) after varied treatments

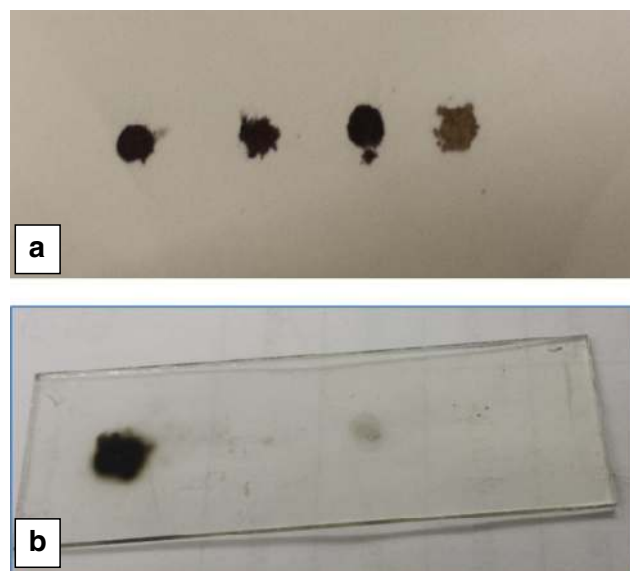| Chemical passivation treatments	Dye reactivity/Resorufin Concentration (μg/mL)
Si-H & APDMES	1.28
Si-H & hydrosilylation	1.13
Si-H & oxidation	1.00
Si-H & APTES	0.79
Si H-annealed & hydrosilylation	0.68
Si-H & oxidation & APDMES	0.18
Si-H & oxidation & APTES	0.02
Sol gel silica (control)	0.02

Fig. 6 **a** photograph **b** chemograph of four samples after 20 hour exposure. (From left to right: Si-H hydrosilylated; Si-H annealed in nitrogen; Si-H APDMES; Si-H APTES)

3 Discussion

Residual chemical reactivity of oxidized porous silicon, as quantified by these specific assays and compared with amorphous silica, could in principle arise from a number of sources that we now discuss in turn. Topics addressed are silicon-hydride bond removal and its re-formation, trace silane emission, trace etch residues, trace solvents, trace metal contamination and the pH microclimate within the pores.

Residual silicon-hydride bonding arrangements are the primary candidate for residual chemical reactivity. Stoichiometric amorphous silica can be rendered more reactive by the introduction of such hydride bonding [31, 32]. Derivatization of porous silicon, by introduction of silicon-carbon bonding, does not remove all such hydride [12, 33], even when side-reactions are minimized [34]. This is generally ascribed to steric hindrance effects [12] but could also be due to some silicon-hydride bonding being within the silicon skeleton, as recently proposed [35]. In this regard, thermal dehydrogenation should be much more effective at removing all silicon-hydride, both surface and internal species. Due to its thermal stability, surface monohydride is reported to require temperatures above 550 °C for its removal. [36] Hydrogen trapped internally by point defects within the skeleton could need temperatures as high as 700 °C [37]. For this reason, samples were oxidized at 700 °C for a long duration and, at least by FTIR, silicon-hydride was reduced to undetectable levels (see Fig. 3b). However, even if silicon-hydride is completely thermally removed, the interaction of residual elemental silicon in the porous

Table 6 Chemography of porous silicon powders (BS419 & BS445) after varied treatments

Chemical passivation treatments	Chemography results
Si-H & hydrosilylation	strong image after 20 hours
Si-H & APTES	faint image after 20 hours; strong image after 72 hours
Si H & APDMES	faint image after 20 hours; stronger image after 100 hrs
Si H- annealed & hydrosilylation	very faint image after 100 hours exposure
Si H , oxidation and APDMES	no image after 100 hours exposure
Si H, oxidation and APTES	no image after 100 hours exposure
Sol gel silica (control)	no image after 100 hours exposure

structure with aqueous environments can lead to its reintroduction. Convincing evidence for silicon-hydride creation from silicon surfaces during alkali etching [38], tribochemical etching in water [39, 40] and storage in weakly alkali solutions like body fluids [41] is available in the literature.

Gaseous silane emission is a second potential source of reactivity [7], especially for biological molecules stored for long periods within the mesoporous structure. Evidence for trace silane emission from both silicon and porous silicon comes from chemography studies [20, 42], FTIR [42, 43] and mass spectrometry [44]. Silane, like surface silicon-hydride bonding, is a potential reducing agent that could react with the two molecular probes used in these assays. Tests where the dye solution was indirectly exposed to silane gas emission from unpassivated porous silicon however were inconclusive, possibly due to its rapid hydrolysis by water during transit [Shabir Q, Loni A. unpublished data]. For the removal of silicon trihydride groups thought to generate monosilane, thermal treatments should be very effective; this is in accord with the nitrogen annealing treatments having a pronounced effect with regard to silane emission (no chemographic image in Fig. 6) but residual monohydride content (residual activity) in both drug assay (Table 4) and dye assay (Table 5).

Trace etch residues, such as silicon tetrafluoride and hexafluorosilicic acid, could potentially introduce chemical reactivity [22]; however, rigorous water and solvent rinsing with multiple exchanges was employed in sample preparation. Fluoride levels in selected batches were undetectable by XRF and XPS [Loni A. unpublished data 45] but the sensitivity of these techniques for this element is not particularly high. Trace solvent levels in selected batches were also quantified and showed ethanol/methanol content at pharmacopeia-acceptable ppm levels (see Table 1).

The primary trace metal contaminants detected were zirconium ~1000 ppm (from the zirconia ball milling process), copper (17-22 ppm) and nickel (11-12 ppm). Arsenic, cadmium, mercury, lead, aluminum, barium, chromium, tungsten, molybdenum, platinum and manganese were all below the detection limit of XRF (Table 1). The presence of zirconium has potential relevance to the final topic discussed next; the surface acidity of oxidized porous silicon.

The pH assays demonstrated that oxidized porous silicon microparticles had lower pH values than commercial silicas prepared by sol-gel technology (e.g. pH 5-7) but comparable values to pharmacopeia-grade fumed silicas like Cab-O-Sil (pH 3.6-4.5). The monomer degradation product, orthosilicic acid, is weakly acidic with a pKa of 9.9 [45]. Polysilicic acids that can arise from hydrolysis-induced supersaturation are stronger acids than the monomer, with pKa values up to 6.5 [45]. One minor contaminant detected in oxidized porous silicon that could influence microclimate pH is zirconium from the ball milling process. Although zirconia is an established biomaterial [46], the incorporation of zirconium into silica is known to increase catalytic activity via Lewis site acidity [47]. Subsequent preliminary tests have shown the drug-based HPLC assay to be strongly pH sensitive, but the dye-based fluorometric assay less so [Webb K, Shabir Q. unpublished data]. Nevertheless all three assays appear to have value in optimizing porous silicon passivation for extended dry and wet storage API stability testing.

Biodegradable porous silicon is currently under assessment as a biomaterial for a wide range of therapeutic medical applications, including brachytherapy, chemotherapy, theranostics and tissue engineering [48]. Its *in-vivo* biocompatibility is the subject of an increasing number of studies [49] but *in-vitro* pharmacopeia-grade testing is also essential for translation of those applications requiring drug delivery into clinical evaluation. We have provided some assays and discussed some issues that should be helpful in this regard.

4 Conclusions

When minimizing the chemical reactivity of porous silicon for drug delivery applications, attention needs to be given to complete removal of silicon hydride bonding, effective rinsing and drying techniques that remove electrolyte components and etch residues, trace metal contamination arising from microparticle batch manufacture and the pH microclimate within the pores. Drug and dye-based storage assays have been developed to quantify residual reactivity. Chemography is currently only a qualitative assay,

but results appear to broadly correlate with the molecular assays. Further research continues to elucidate the causes of residual chemical reactivity, as monitored by these sensitive assays, and the extent to which the data correlates with model API stability during lengthy storage.

References

1. Prestidge CA, Barnes TJ, Lau CH, Barnett C, Loni A, Canham LT (2007) Mesoporous silicon : a platform for the delivery of therapeutics. Expert Opin Drug Deliv 4(2):101–110

2. Salonen J, Kaukonen AM, Hirvonen J, Lehto VP (2008) Mesoporous silicon in drug delivery applications. J Pharm Sci 97(2):632–653

3. Anglin EJ, Cheng L, Freeman WR, Sailor MJ (2008) Porous silicon in drug delivery devices and materials. Adv Drug Deliv 60(11):1266–1277

4. Shahbazi MA, Herranz B, Santos HA (2012) Nanostructured porous Si-based nanoparticles for targeted drug delivery. Biomatter 2(4):296–312

5. Barnes TJ, Jarvis KL, Prestidge CA (2013) Recent advances in porous silicon technology for drug delivery. Ther Deliv 4(7):811–823

6. Martín-Palma RJ1, Hernández-Montelongo J, Torres-Costa V, Manso-Silván M, Muñoz-Noval Á (2014) Nanostructured porous silicon-mediated drug delivery. Expert Opin Drug Deliv 11(8):1273–1283

7. Canham LT (1995) Bioactive silicon fabrication via nanoetching techniques. Adv Mater 7:1033

8. Park JH, Gu L, Von Maltzahn G, Ruoslahti E, Bhatia SN, Sailor MJ (2009) Biodegradable luminescent porous silicon nanoparticles for in-vivo applications. Nat Mater 8(4):331–336

9. Shabir Q (2014) Biodegradability of porous silicon. In: Canham L (ed) Handbook of Porous Silicon. Springer, Switzerland, pp 235–236

10. Khokhlov A, Valiullin R. (2014) Mesoporous silicon. In: Canham L (ed) Handbook of Porous Silicon. Springer, Switzerland, pp 123–145

11. Wan Y, Apostolou S, Dronov R, Kuss B, Voelcker NH (2014) Cancer-targeting siRNA delivery from porous silicon nanoparticles. Nanomedicine 9(15):2309–2321

12. Sailor MJ (2014) Chemical reactivity and surface chemistry of porous silicon. In: Canham L (ed) Handbook of Porous Silicon. Springer, Switzerland, pp 355–380

13. De Stefano L, Oliviero G, Amato J, Borbone N, Piccialli G, Mayol l, Rendina I, Terracciano M, Rea I (2013) Aminosilane functionalization of mesoporous oxidized silicon for oligonucleotide synthesis and detection. J Royal Soc Interface 10:20130160

14. Nadarassan DK, Loni A, Shabir Q, Kelly C, O'Brien H, Caffull E, Webb K, Canham LT, Maniruzamman M, Trivedi V, Douroumis D (2015) Ultrahigh drug loading and release from biodegradable porous silicon aerocrystals. Extended Abstract No. 825 42nd Meeting of Controlled Release Society. 26-29th July Edinburgh, UK

15. Estey T, Kang J, Schwendeman SP, Carpenter JF (2006) BSA degradation under acidic conditions: a model for protein instability during release from PLGA delivery systems. J Pharm Sci 95(7):1626–1639

16. Agrawali CM, Athanasiou KA (1997) Technique to control pH in vicinity of biodegrading PLA-PLGA implants. J Biomed Mater Res 38(2):105–114

17. Kuhlmann J, Bartsch I, Willbold E, Schuchardt S, Holz O, Hort N, Höche D, Heineman WR, Witte F (2013) Fast escape of hydrogen from gas cavities around corroding magnesium implants. Acta Biomater 9(10):8714–8721

18. Song GL, Song SZ (2006) Corrosion behaviour of pure magnesium in a simulated body fluid. Acta Phys Chim Sin 22(10):122–126

19. Emmanuel B, Thomas E, Annette B, Gabriele L, Helmut L, Heinrich W (2005) Reference values for serum silicon in adults. Anal Biochem 337:130–135

20. Jay T, Canham LT, Heald K, Reeves CL, Downing R (2000) Autoclaving of porous silicon within a hospital environment: potential benefits and problems. Phys Stat Solidi A 182(1):555–560

21. Riikonen J, Salomäki M, van Wonderen J, Kemell M, Xu W, Korhonen O, Ritala M, MacMillan F, Salonen J, Lehto VP (2012) Surface chemistry reactivity and pore structure of porous silicon oxidized by various methods. Langmuir 28:10573–10583

22. Koynov S, Pereira RN, Crnolatac I, Kovalev D, Huygens A, Chirnovy V, Stuzmann M, de Witte P (2011) Purification of nano-porous silicon for biomedical applications. Adv Engn Mater 13(6):B225–B233

23. Loni A (2014) Porous silicon formation by anodization. In: Canham L (ed) Handbook of Porous Silicon. Springer, Switzerland, pp 11–22

24. Terracciano M, Rea I, De Stefano L, Rendina I, Oliviero G, Nici FD, Errico S, Piccialli G, Borbone N (2014) Synthesis of mixed sequence oligonucleotides on mesoporous silicon: chemical strategies and material stability. Nanoscale Res Lett 9:317

25. Krishnamohan T, Ialitha G, Sharma RV, Sambasivarao L, Babu JM, Younus M, Raju AS, Murthy YLN (2012) Method development and validation for estimation of related compounds present in lansoprazole bulk drug by ultra high pressure liquid chromatography. Asian J Res Chem 5(7):859–865

26. O'Brien J, Wilson I, Orton T, Pognan F (2000) Investigation of the Alamar Blue (resazurin) fluorescent dye for the assessment of mammalian cell cytotoxicity. Eur J Biochem 267:5421–5426

27. Low SP, Williams KA, Canham LT, Voelcker NH (2006) Evaluation of mammalian cell adhesion on surface-modified porous silicon. Biomaterials 27:4538–4546

28. Canham LT, Saunders SJ, Healey PB, Keir AM, Cox T1 (1994) Rapid chemography of porous silicon undergoing hydrolysis. Adv Mater 6(11):865–868

29. Buriak JM, Stewart MP, Geders TW, Allen MJ, Choi HC, Smith JD, Raftery D, Canham LT (1999) Lewis acid mediated hydrosilylation on porous silicon surfaces. J Am Chem Soc 121(49):11491–11502

30. Lansoprazole Monograph (2006) United States Pharmacopeia. USP 29 NF24: 1229

31. Vella E, Buscarino G, Boscaino R (2011) Structural organization of silanol and silicon hydride groups in the amorphous silicon dioxide network. Eur Phys J B 83:47–52

32. Claudio M, Manfred JDL (1969) Reactive Silica II The Nature of the Surface Silicon Hydrides. J Phys Chem 73(2):327–333

33. Huck LA, Buriak JM (2014) Silicon-carbon bond formation on porous silicon. In: Canham L (ed) Handbook of Porous Silicon. Springer, Switzerland, pp 683–693

34. Boukherroub R, Petit A, Loupy A, Chazalviel JN, Ozanam F (2003) Microwave –assisted chemical functionalization of hydrogen-terminated porous silicon surfaces. J Phys Chem 107(48):13459–13462

35. Loni A, Canham LT (2013) Exothermic phenomena and hazardous gas release during thermal oxidation of mesoporous silicon powders. J Appl Phys 113:173505
36. Gupta P, Colvin VL (1988) George SM.Hydrogen desorption kinetics from monohydride and dihydride species on silicon surfaces. Phys Rev B 37(14):8234–8243
37. Stein HJ (1975) Bonding and thermal stability of implanted hydrogen in silicon. J Electronic Mater 4(1):159–174
38. Wind RA, Jones H, Little MJ (2002) Hines MA Orientation-Resolved Chemical Kinetics: Using Microfabrication to Unravel the Complicated Chemistry of KOH/Si Etching. J Phys Chem B106(7):1557–1569
39. Mizuhara K, Hsu SM Tribochemical reaction of oxygen and water on silicon surfaces. In: Dowson D (ed) Wear Particles.1992; Elsevier Science Publishers B. V. p 323
40. Muratov VA, Olsen JE, Gallois BM, Fischer TE, Bean JC (1998) Tribochemical Reactions of Silicon: An in Situ Infrared Spectroscopy Characterization. J Electrochem Soc 145(7):2465–2470
41. Ulin V, Ulin N, Soldatenkov F, Semenov A, Bobyl A (2014) Surface of porous silicon under hydrophilization and hydrolytic degradation. Semiconductors 48(9):1211–1216
42. Lampert I, Fußstetter H, Jacob H (1989) Evidence for SiH4 Formation during the Reaction of Water with a Silicon Surface. J Electrochem Soc 133(7):1472–1474
43. Salonen J, Lehto VP, Laine E (1997) The room temperature oxidation of porous silicon. Appl Surf Sci, 191–198
44. Gunasingham PV, Goldspink G (2000) An investigation into silane evolution from porous silicon by temperature programmed desorption method. J Porous Mater 7:187–190
45. Iler RK (1979) The Chemistry of Silica: solubility, polymerization, colloid and surface properties and biochemistry. Wiley, New York
46. Piconi C, Maccauro G (1999) Zirconia as a ceramic biomaterial. Biomaterials 20:1–25
47. Rodríguez-Castellóna E, Jiménez-Lópeza A, Maireles-Torresa P, Jonesb PD, Rozièreb J, Trombettac M, Buscac G, Lenardad M, Storarod L (2003) Textural and structural properties and surface acidity characterisation of mesoporous silica-zirconia molecular sieves. J Solid State Chem 175:159–169
48. Santos H (ed.) (2014) Biomedical Applications of Porous Silicon, Woodhead Publishing
49. Low SP, Voelcker NH Biocompatibility of porous silicon. In: Canham L (ed) Handbook of Porous Silicon, pp 381–393